

Structural properties of hot wire *a*-Si:H films deposited at rates in excess of 100 Å/s

A. H. Mahan^{a)} and Y. Xu

National Renewable Energy Laboratory (NREL), Golden, Colorado 80401

D. L. Williamson

Department of Physics, Colorado School of Mines, Golden, Colorado 80401

W. Beyer

Forchungszentrum Julich, Julich, Germany

J. D. Perkins

National Renewable Energy Laboratory (NREL), Golden, Colorado 80401

M. Vanecek

Institute of Physics, Academy of Sciences of the Czech Republic, Prague 6, Czech Republic

L. M. Gedvilas, and B. P. Nelson

National Renewable Energy Laboratory (NREL), Golden, Colorado 80401

(Received 11 June 2001; accepted for publication 2 August 2001)

The structure of *a*-Si:H, deposited at rates in excess of 100 Å/s by the hot wire chemical vapor deposition technique, has been examined by x-ray diffraction (XRD), Raman spectroscopy, H evolution, and small-angle x-ray scattering (SAXS). The films examined in this study were chosen to have roughly the same bonded H content C_H as probed by infrared spectroscopy. As the film deposition rate R_d is increased from 5 to >140 Å/s, we find that the short range order (from Raman), the medium range order (from XRD), and the peak position of the H evolution peak are invariant with respect to deposition rate, and exhibit structure consistent with a state-of-the-art, compact *a*-Si:H material deposited at low deposition rates. The only exception to this behavior is the SAXS signal, which increases by a factor of ~ 100 over that for our best, low H content films deposited at ~ 5 Å/s. We discuss the invariance of the short and medium range order in terms of growth models available in the literature, and relate changes in the film electronic structure (Urbach edge, as-grown defect density) to the increase in the SAXS signals. We also note the invariance of the saturated defect density versus R_d , measured after light soaking, and discuss possible reasons why the increase in the microvoid density apparently does not play a role in the Staebler–Wronski effect for this type of material. © 2001 American Institute of Physics. [DOI: 10.1063/1.1407317]

INTRODUCTION

During the last several years, an intense effort has been initiated to raise the deposition rate (R_d) of hydrogenated amorphous silicon *a*-Si:H films without sacrificing material quality.¹ The *a*-Si:H grown for industrial purposes is typically grown at R_d 's from 1 to 3 Å/s, and most of the viable manufacturing processes still grow *a*-Si:H at rates below 10 Å/s.² The ability to grow films at higher rates with a preservation of both material and device performance would not only reduce the industry's up-front and total capital equipment costs, but would also reduce materials (source gas) expenditures. To date, little information is available on the electronic and structural properties of high R_d films, and those that do exist are mainly on films prepared by new and/or novel deposition techniques which have not yet been adopted by industry. When high R_d deposited films have been incorporated into devices (solar cells), the results has typically been that not only does the initial device performance be-

come inferior, but also the light induced metastability, or Staebler–Wronski effect (SWE), increases.³ It is, therefore, an open scientific question as to whether a significant increase in R_d can be accompanied by a preservation of state of the art structural and electronic film properties as well as device performance.

In previous studies related to *a*-Si:H deposited by the hot wire chemical vapor deposition (HWCVD) technique, a 9.8% device efficiency for a laboratory device was reported with the *i* layer deposited at 16.5 Å/s;⁴ this remains a record initial efficiency for a device whose *i* layer was deposited at this (high) rate. The electronic properties of these films, including the saturated defect densities, have been reported elsewhere.⁵ More recently, the first results were presented on the electronic properties of HWCVD films deposited at much higher rates (up to 150 Å/s) using multiple W filaments.^{6,7} In these articles, it was shown that a light/dark conductivity ratio of $> 10^5$ could be preserved up to R_d 's exceeding 130 Å/s. Further, while the initial state defect densities did increase gradually with increasing R_d , the saturated (light-soaked) defect densities remained invariant over this entire

^{a)} Author to whom correspondence should be addressed; electronic mail: hmahan@nrel.gov

TABLE I. Deposition conditions and selected material properties (film C_H , conductivity values) for films used in this study.

Film No.	Deposition rate ($\text{\AA}/\text{s}$)	Filament No. spacing (cm)	$T_{S(\text{init})}$ ($^{\circ}\text{C}$)	P_{ch} (mT)	SiH_4 flow (sccm)	I (Amps) per filament	C_H (at. %)	σ_1, σ_d (S/cm^2)
HW47	6	1/5	380	10	20	15	2.3	4.2×10^{-6} , 6.9×10^{-12}
L016	17	1/5	302	17	75	16	6.3	1.7×10^{-5} , 4.8×10^{-11}
L043	34	2/4	300	20	50	15	6.6	1.7×10^{-5} , 5.3×10^{-11}
L032	40	2/5	325	45	50	15	2.7	7.8×10^{-6} , 4.4×10^{-10}
L113	71	2/3.2	315	35	50	15	7.3	8.5×10^{-5} , 4.6×10^{-10}
L103	87	2/3.2	315	50	50	15	10	5.7×10^{-5} , 5.3×10^{-10}
L117	94	2/3.2	316	50	75	15	6.8	3.5×10^{-5} , 2.7×10^{-10}
L095	109	2/3.2	400	50	75	15	7.1	5.4×10^{-5} , 1.1×10^{-9}
L106	111	2/3.2	350	50	75	15	8.0	3.9×10^{-5} , 5.0×10^{-10}
L105	114	2/3.2	350	50	75	15	7.7	3.7×10^{-5} , 2.8×10^{-10}
L093	124	2/3.2	385	70	75	15	4.7	3.2×10^{-5} , 5.4×10^{-10}
L192	132	2/3.2	326	70	75	15	6.4	2.1×10^{-5} , 2.0×10^{-10}
L096	144	2/3.2	385	90	75	15	6.4	2.2×10^{-5} , 4.6×10^{-10}

range of R_d 's ($1.5-4 \times 10^{16} \text{ cm}^{-3}$), and approach those of the best HWCVD material grown at 5–8 $\text{\AA}/\text{s}$.

In this article, we describe the first detailed results on the structural properties of these HWCVD films deposited at very high R_d 's. The films examined in this study were chosen to have roughly the same bonded H content (C_H). Under these conditions, the structural ordering of these films, as probed by x-ray diffraction (XRD), Raman, and H evolution measurements, remain almost completely unchanged with increasing R_d , and again approach those of the best HWCVD material grown at 5–8 $\text{\AA}/\text{s}$. The only exception to this (invariant) structural behavior is a sizeable increase in the amount of small angle x-ray scattering (SAXS), which is a measure of the film inhomogeneity typically associated with microvoids.⁸ We discuss the invariance of the film structural order with increasing R_d in the context of growth models for α -Si:H, and the possible effects of this increasing microvoid density on both the Urbach edge and the (initial, saturated) defect densities reported earlier.

EXPERIMENT

In this work we used the same, isothermally heated HWCVD deposition reactor in which the device work was previously done,⁵ but this time using two parallel W filaments heated to ~ 2000 $^{\circ}\text{C}$, where the filament/substrate spacing was varied between 3.2 and 5.0 cm. When we decreased this spacing from the 5.0 cm value used previously, the distance between the filaments was also changed to en-

sure reasonable film thickness uniformity over substrate area (4 cm \times 2.5 cm). Depositions were made simultaneously on 1737 Corning glass, *c*-Si, and stainless steel (SS) substrates; in contrast to the HWCVD *i* layers used in device fabrication,^{4,9} the present films were pulled into the load-lock immediately after deposition, and were cooled rapidly in an Ar atmosphere. Using the light/dark conductivity ratio as a preliminary gauge of material quality, we identified a series of films of similar (~ 1 μm) thickness and H content which spanned the deposition range between 18 and 144 $\text{\AA}/\text{s}$. While the conductivity ratio was observed to decrease with increasing R_d , ratios $> 10^5$ were nevertheless achieved for R_d 's as high as 133 $\text{\AA}/\text{s}$. The major factors contributing to the increase in R_d were the change from one to two filaments and the decrease in filament/substrate spacing. To preserve material quality at the decreased spacing, the deposition chamber pressure and substrate temperature, and to some extent the silane flow, were increased.⁶ The deposition parameters for these films are shown in Table I. We note that the C_H 's of these films, as obtained from infrared spectroscopy, ranged primarily between 6 and 8 at. %. Infrared data for a typical high HWCVD R_d film (deposited at 114 $\text{\AA}/\text{s}$) are shown in Fig. 1. Within the detectability limits probed by the infrared technique, such films do not contain any bonded H exhibiting an infrared signature at 2100 cm^{-1} . For the constant photocurrent measurement (CPM) and conductivity measurement, Cr coplanar contacts were evaporated onto the films. On some films variable spacings were used to characterize

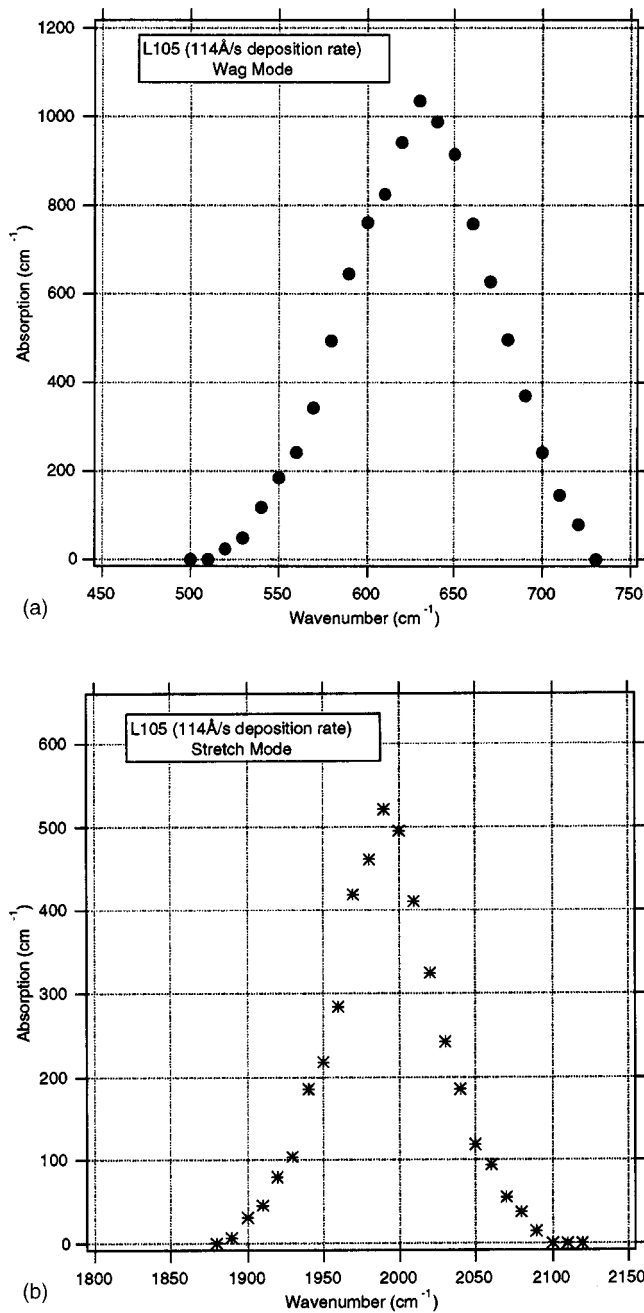


FIG. 1. Infrared absorption spectra, for a film deposited at 114 \AA/s , showing absorption in regions corresponding to: (a) the Si-H wag mode and (2) the Si-H stretch mode.

the light scattering effects and to correct the measured data for light scattering.¹⁰ To obtain structural information, the medium range order (MRO) was determined by XRD from the width of the first diffraction peak for the samples deposited on SS,¹¹⁻¹³ while the short range order (SRO) was obtained by Raman spectroscopy, for films deposited on the glass substrates, from the half width at half maximum (HWHM) on the high wave number side of the amorphous Si-Si transverse optical peak centered at $\sim 480 \text{ cm}^{-1}$.¹⁴ The invariance of Raman data for thick films deposited on different substrates has been noted.¹⁵ H evolution measurements on selected samples deposited on *c*-Si also provided information on the structural properties versus the R_d increase.¹⁶

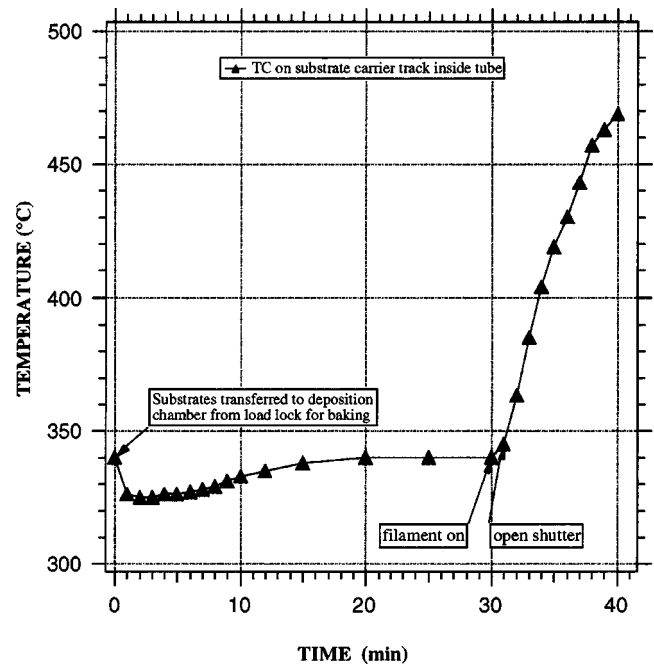


FIG. 2. T_s vs time after loading a substrate (no film) into the deposition chamber.

In separate depositions using identical deposition conditions, films were deposited either on high purity, $10\text{-}\mu\text{m}$ -thick Al foil or thin ($\sim 70 \mu\text{m}$) Si wafers for SAXS measurements.⁸ Since an isothermal chamber was used for all depositions, careful clamping of the Al foil around a SS substrate, needed to ensure that the foil reaches the desired temperature when an external substrate heater is used, is not crucial here. We comment that the films deposited on the Si wafers give SAXS results similar to those deposited on the Al foil, and that XRD showed no evidence of Al-induced crystallization on any of the SAXS samples. To investigate whether the increased SAXS intensity was due to either the increase in R_d or the doubling of filaments used for the (higher rate) depositions, films were deposited using either one or two filaments at the same R_d . In the one notable exception to the (constant) film C_H mentioned above, a low C_H (2 at. %) HWCVD film deposited at $\sim 5 \text{ \AA/s}$ using a single filament is included in the SAXS data, as it plays an important role in the discussion that follows.

We note that the substrate temperatures of our films, as monitored by thermocouples mounted at various positions within the isothermal deposition chamber, increase with time during deposition. This is due to exposure of the growing film surface to radiation from the filament(s). This increase in temperature with exposure time is shown in Fig. 2, with the temperature of the isothermal chamber set at $335 \text{ }^\circ\text{C}$. While the increase in temperature is minimal for the $\sim 2000 \text{ \AA}$ thick layers typically used in device fabrication ($\sim 5 \text{ }^\circ\text{C}$ rise in 20 s for a deposition rate of 100 \AA/s), it may rise more than $60\text{--}70 \text{ }^\circ\text{C}$ in the time needed to deposit a $1\text{-}\mu\text{m}$ -thick film at high R_d 's. Therefore, because of this substrate temperature increase with deposition time, the temperatures given in Table I reflect the initial set temperatures of the

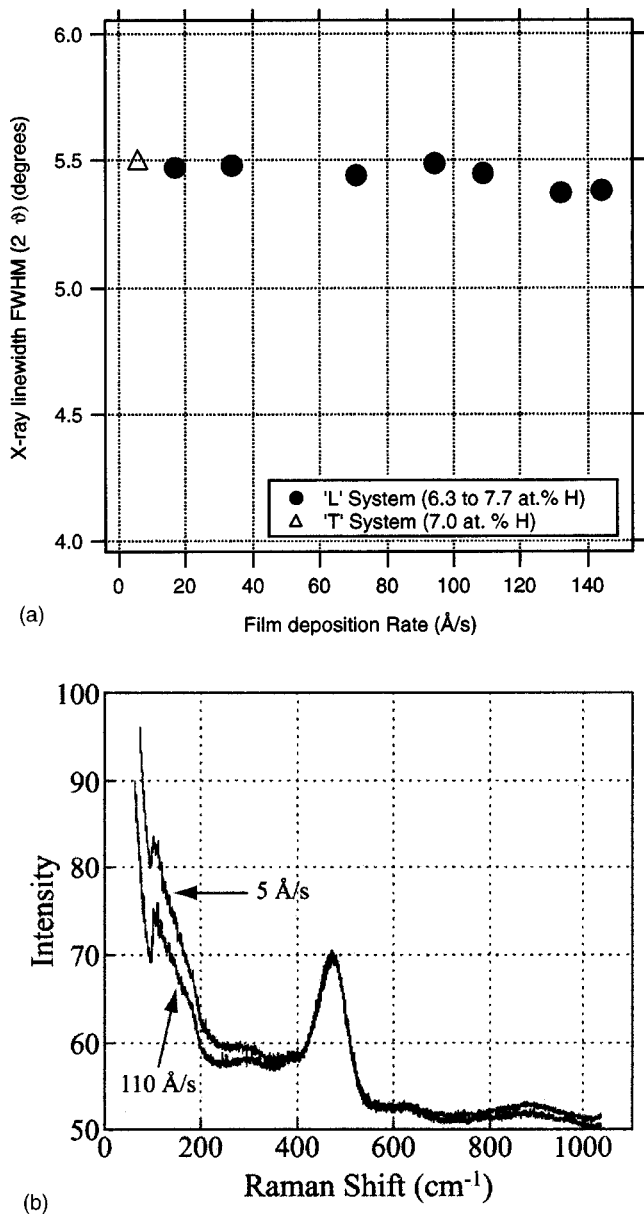


FIG. 3. (a) X-ray linewidth FWHM (2θ) vs film R_d . The deposition systems used to deposit which films are indicated, and are described in Ref. 5; (b) Raman spectra for films deposited at 5 and 110 Å/s, respectively.

isothermal chamber (before the substrate is exposed to radiation from the filament).

RESULTS

Figure 3 shows the results of (a) the XRD and (b) Raman measurements on the HWCVD deposited films as a function of increasing R_d . While the XRD peak widths ($2\theta \sim 5.4^\circ - 5.5^\circ$) lie approximately midway between the value for plasma enhanced CVD (PECVD) a -Si:H deposited without H dilution and the narrowest value measured to date for a fully amorphous sample,^{11,12} the values are invariant as the R_d is increased from 18 to 144 Å/s. A similar FWHM [Fig. 3(Δ)] is also observed for a film containing ~ 7 at. % H which was deposited at ~ 6 Å/s using a single filament placed 5 cm from the substrate. The same (invariant) trend is seen in the Raman measurements for two HWCVD films

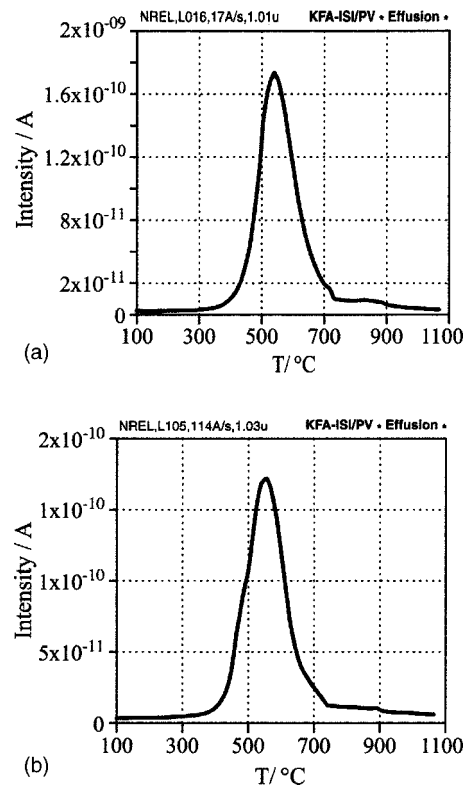


FIG. 4. H effusion spectra for HWCVD films deposited at R_d 's of 17 and 114 Å/s, respectively. The temperature ramp rate is noted.

deposited at widely different R_d 's (5 and 110 Å/s). In particular, the HWHM on the high wave number side of the Si-Si transverse optical mode is also invariant as R_d is increased to >100 Å/s. We note that the HWHM values in Fig. 3(b) (~ 32 cm⁻¹) are close to the narrowest values reported in the literature for a -Si:H.^{11,15,17}

In Fig. 4, we show H effusion results for two films: one deposited at the rate recently explored in device fabrication (17 Å/s) using one filament^{4,5,18} and the other at 114 Å/s using two filaments. In compact a -Si:H, only one evolution peak is observed, whose position varies with film thickness; for a 1 μm thick film, this position is roughly at 550 °C.¹⁶ As can be seen, the peak position for the 17 Å/s film is identical to this value, and all other measurements on this film are consistent with a compact material. The low C_H (1–2 at. %) films, deposited at 4–8 Å/s, also exhibit spectra identical to the one for the 17 Å/s film shown in Fig. 4.¹⁹ Turning to the data for the higher (114 Å/s) R_d film, we also observe the existence of only one evolution peak, with its peak position close to that for the 17 Å/s film, but approximately 15 °C higher in temperature. Such a feature again is indicative of a compact material. We do note the existence of a small shoulder on the low temperature side of the main peak. We do not believe this feature indicates the existence of some additional microstructure; rather, it is most likely due to the formation of pinholes (blisters) during the effusion process.²⁰

In Fig. 5(a) we show SAXS data for our films, once again plotted versus R_d . The integrated SAXS intensity (Q_N) is due to nanostructural features.⁸ Here, in contrast to Figs. 3 and 4, there is a clear distinction between our low

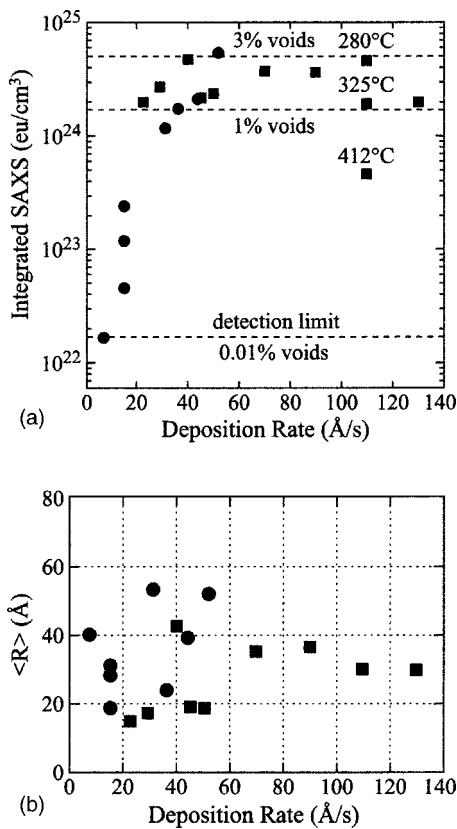


FIG. 5. (a) Integrated SAXS intensity vs film R_d ; (b) microvoid radius vs film R_d . The symbols (●) and (■) refer to films deposited using one and two filaments respectively, with the initial T_s 's, unless otherwise indicated, between 300 and 350 °C.

deposition rate, low C_H films (~ 5 Å/s) with a very low microvoid density ($\sim 0.01\%$, which is near the detection limit of the SAXS technique) and all of our high R_d films deposited with either one or two filaments (but with varying filament/substrate spacing). Indeed, it is seen that all our high R_d (> 20 Å/s) films exhibit integrated SAXS intensities that correspond to apparent microvoid volume fractions (V_f) in the range of $\sim 1\%$ – 3% . While we note on the one hand that V_f can be reduced for the high R_d films by increasing the substrate temperature (see Fig. 5), these SAXS V_f 's for the high deposition rate films identified for this structural study (deposited at constant initial temperature) are again nearly independent of R_d . The observed slight variations, which are often outside the experimental uncertainty of about 10% for these high Q_N films, can be attributed to differences in preferred orientation of a columnar-like microstructure, as detected by tilting the films relative to the x-ray direction.⁸ In particular, the observed reductions in Q_N upon 45° tilting range from factors of 3–10, indicating significantly oriented features. This also means that the indicated V_f 's may be too high by factors of about 2.5–5, based upon an ellipsoidal shape. In Fig. 5(b) we show measurements of the microvoid radius versus R_d . As can be seen, this radius, measured in the plane of the film, is fairly large and is also roughly independent of film R_d , ranging roughly from 20 to 50 Å.

Finally, we plot in Fig. 6(a) the optical absorption coefficient spectra as measured by CPM, and (b) the slope of the

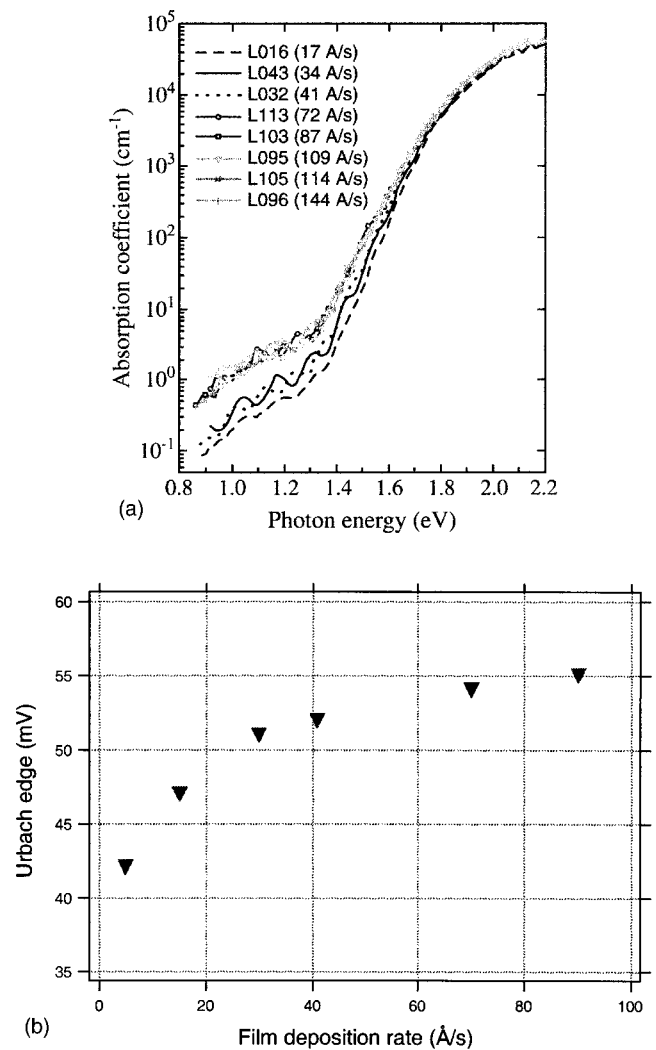


FIG. 6. (a) CPM absorption spectra for selected samples, with R_d ranging between 17 and 144 Å/s; (b) E_0 , obtained from the slope of the CPM spectra vs R_d .

exponential Urbach edge E_0 versus film R_d . As can be seen, both the optical absorption in the subgap, defect-connected region around (α) at 1.2 eV and the slope E_0 increase with increasing R_d . In the case of the Urbach edge [Fig. 6(b)], E_0 increases from a value of 42 mV for (low H content) HWCVD films deposited at ~ 4 – 8 Å/s,²¹ to ~ 55 mV for films deposited at 87 Å/s. From Fig. 6(a), the E_0 slopes for the films deposited at an $R_d > 87$ Å/s are indistinguishable from each other, indicating a saturation in E_0 versus R_d ; hence, these (saturated) values for $R_d > 100$ Å/s are not shown in Fig. 6(b).

A comparison of the present structural results with those of other high R_d a -Si:H is sketchy at best, due to the lack of research and/or publications regarding this subject. Those that are available are data from a -Si:H deposited by the expanding thermal plasma (ETP) technique. In particular, for ETP a -Si:H deposited at ~ 70 Å/s, the Raman $\Gamma/2$ is 33 cm⁻¹, the Urbach edge E_0 is 53 mV, and while the ETP film exhibits a C_H similar to that of the present HWCVD films (~ 6 – 8 at. %), the infrared parameter R^* is ~ 0.20 .²² The definition of R^* ($= [2070]/([2070] + [2000])$), and its asso-

ciation with some type of microstructure, is discussed elsewhere.²³

DISCUSSION

We first comment on the preservation of ordering parameters (Figs. 3–4) with increasing HWCVD R_d . We do this in the context of growth models available in the literature. Models of film growth have evolved considerably in the last 20 yrs. Although the first model (using a thermodynamic approach) was indeed successful in explaining a variety of experimental results (such as the E_0 and defect densities),²⁴ they were not very explicit in explaining how film growth took place, and so will not be used here. More appropriate to this discussion is the model of Matsuda, Gallagher, and Perrin (the MGP model),^{25–27} which discusses film growth in the presence of the SiH_3 growth precursor. The central assumption of this model is the existence of a weakly adsorbed (physisorbed) state, allowing the SiH_3 radical to diffuse over the surface with a low sticking coefficient, and thus be incorporated “in well spaced and coordinated sites;”²⁵ in other words, at sites of optimum structural order, presumably as measured by Raman (and XRD). We note that when this growth model is applied to device quality PECVD a -Si–H (deposited, e.g., at 1–3 Å/s), grown at standard substrate temperatures, what results structurally is a film possessing optimum structural parameters similar to those seen in Figs. 3–4.^{8,15} Turning now to HWCVD, the growth precursor(s) of a -Si:H grown at 4–8 Å/s have also been investigated,^{28,29} and in this case SiH_3 was also determined to be the predominant radical growth specie. From the above discussion, this also leads to films with optimum structural properties, as seen in Figs. 3–4. The invariance of the structural properties of the present films with R_d (up to rates exceeding 100 Å/s) leads us to suggest that the present high R_d HWCVD films must also be deposited with SiH_3 as the main gas precursor specie. Along these lines, we note that Kessels arrived at the same conclusion for the high R_d ETP a -Si:H,²² and the similar Raman $\Gamma/2$ values observed for the high R_d films lend additional support to the suggestion that SiH_3 is the predominant radical contributing to film growth in the present HWCVD case.

On the other hand, while SiH_3 may be the dominant gas phase Si-containing specie contributing to film growth, in contrast to the MGP model it may not be the only gas Si specie. That is, secondary species may exist which play a role in the microvoid formation that is present at high HWCVD R_d 's, even for a film which otherwise exhibits optimum structural order. This is due to the following argument. For HWCVD a -Si:H deposited at low rates (4–8 Å/s), the gas depletion is estimated to be similar to that for device quality PECVD a -Si:H (10%–25%), and hence there is ample SiH_3 in the gas ambient (through the gas phase reaction $\text{H} + \text{SiH}_4 \rightarrow \text{SiH}_3 + \text{H}_2$)²⁸ to contribute to film growth. It is worth noting once again that these films, deposited with SiH_3 as the predominant gas phase Si precursor, exhibit the lowest SAXS microvoid density measured in the literature to date for a -Si:H.⁸ However, for HWCVD films deposited at rates >50 – 60 Å/s, the gas is considerably more depleted than

before ($>70\%$ for a film deposited at an $R_d \sim 60$ Å/s.)⁷ Although the structural measurements suggest that SiH_3 is still the dominant Si containing radical contributing to film growth, this increased gas depletion has several consequences. We argue that the atomic H will still react with most of the available SiH_4 to produce SiH_3 in the usual manner. The question is what happens to the Si that is also evaporated (besides the atomic H) from the filament under the high filament temperature conditions. Since the mechanisms that enabled the “disappearance” or “neutralization” of Si also involved its reaction with SiH_4 ,²⁸ it is possible that a small flux of Si atoms could also reach the growing surface and thus contribute to film growth, since such reactions (which “eliminate” Si) would also be reduced due to the higher SiH_4 depletion. Therefore, while awaiting definitive experimental results in this regard, we suggest that growth of HWCVD a -Si:H at high rates is still dominated by the SiH_3 precursor, but with the possibility of minor (Si) species contributing in some fashion.

We next attempt to link microvoid formation to this different mix of radical species. Microvoid formation has been a puzzle for those modeling a -Si:H growth. In the MGP model (with SiH_3 as the only gas precursor), it is suggested³⁰ that film surface smoothness (along with the consequent lack of microvoid formation) does not naturally follow from the surface diffusion of SiH_3 only. This can be seen from the fact that since dangling bond (DB) creation is random on the film surface, film growth will also be random, as the SiH_3 radicals can only stick at these (randomly positioned) DB sites. If, on the other hand, any uneven film growth has previously occurred, such as that caused, i.e., by island formation in the initial stages of film growth, then the SiH_3 's would need to have a higher probability of finding DBs in the film valleys to ensure surface smoothness; from the model, this does not happen. Consequently, any uneven film growth, once started, would be accentuated with growing film thickness, leading to resultant shadowing and probable microvoid growth. Avoidance of these shadowing effects is usually argued in models, by, i.e., surface diffusion of DB's,³¹ enabling them to gather at the film steps and valleys of the growing film surface, with the consequent growth at these areas which would otherwise not be accentuated.

On the other hand, it is easier to evoke microvoid formation if some (small percentage of) growth precursors have a high sticking coefficient. Such precursors will obviously stick where they land on the film surface, and growth from such species has been shown previously to contribute to inferior film quality, both in a structural as well as in an electronic sense.^{25,32} Following the argument of Berntsen, but for a different precursor,¹⁵ we propose that (from the above) the large majority of film growth of the present high R_d films is dominated by SiH_3 precursors, and that microvoid formation is enhanced at places where precursors with a low surface mobility (Si) attach to a surface atom. Consequently, the overall structure of the bulk material is still determined by the high surface mobility of the predominant SiH_3 radicals, and the microvoid volume fraction is determined by the (small) Si radical flux hitting the film surface.

In all prior discussions about film growth in this article, the assumption has been made that the growing film surface is saturated with H. For the low R_d HWCVD case discussed above, we see no reason to deviate from this assumption, due to the excellent agreement between the MGP growth model (assuming only SiH_3 radical film growth) and the state of the art structural properties exhibited by these low R_d films^{8,11} which are consistent with this model. On the other hand, due to the high gas phase depletions, film growth at high R_d may be a different matter. In addition to the (small) flux of Si atoms that may contribute to microvoid formation, there is also the issue of an atomic H flux to consider. In particular, not only may a portion of the unreacted Si flux reach the growing film surface (and contribute to microvoid formation, as discussed above), but a considerably larger flux of unreacted H atoms may reach the growing film surface as well. How this impinging atomic H affects the growing film surface is a matter of conjecture. If the H abstraction reaction (by H) is important,³³ then more surface dangling bonds would be created than in the low R_d HWCVD case; this in turn would not only “free up” more surface sites to enable faster film deposition, but would also suggest a reduction in the surface mobilities of the major Si containing radical species (primarily SiH_3) that contribute to (this faster) film growth. Were this to occur, the MGP model would predict that films with poorer structure would result. However, at least from the present high R_d structural measurements (Raman, XRD, H evolution) this is not the case, as the results of such measurements are consistent with films of optimum structural quality. From this observation, we can draw two distinctly disparate conclusions. The first is that the structural measurements are relatively insensitive to the magnitude of the surface diffusion of the impinging Si radical species (SiH_3 and/or Si) if H does indeed abstract surface H in a manner claimed above since, as mentioned above, these measurements are consistent with a film of optimal structural quality. The second conclusion is that, in addition to the H abstraction reaction, the impinging H could also etch the weak surface bonds created by the lower surface mobilities of the impinging Si-containing radicals, thus preserving the structural integrity of the growing films (as measured by Raman, XRD, and H evolution).

Regarding the issue of the source of the decreased H surface coverage, it has also been suggested that, at the high T_s 's used for the high R_d HWCVD films, H thermal desorption would begin to occur,³³ leading to additional surface DB formation and possibly higher microvoid volume fractions. We discount such a H desorption related microvoid formation process for two reasons. First, low deposition rate (4–8 Å/s), low H content (1–2 at. %) HWCVD films have been deposited at similar (high) film T_s 's (~380–400 °C), and exhibit SAXS signals at the detection limit for a -Si:H (~0.01% microvoids).⁸ And second, should H thermal desorption play a significant role in microvoid formation, then depositing films at even higher T_s (400–500 °C) should result in increased SAXS signals. However, from Fig. 5 this is not the case, as the film series deposited at ~100 Å/s at varying T_s show a reduction in the SAXS intensities as the film T_s is increased.

We now address the issue of the cause of the increase in E_0 with increasing film R_d , as seen in Fig. 6. It is generally agreed that with increasing bond disorder, the density of strained bonds, as reflected in E_0 , increases.³⁴ The cause of this increased disorder has again been the subject of debate. In the thermodynamic models, H certainly mediates the strained bond to broken bond reaction process, with the minimum disorder limited by network constraints (thermal disorder),³⁴ but again no specific mechanism was presented. Schubert *et al.*¹⁷ then examined E_0 versus $\Gamma/2$ for a wide variety of film systems (a -Si:H, a -SiN:H, a -SiC:H), and although correlations were observed between an increasing Raman $\Gamma/2$ (increased bond disorder) and an increasing E_0 , no unique correspondence was observed. Also observed were very different data for PECVD a -SiC:H, where E_0 broadened significantly without any widening of $\Gamma/2$. Different types of film microstructure were suggested to be the cause of this nonuniqueness, but no specific details regarding this microstructure were given. As an aside, we note that the anomalous data for the PECVD a -SiC:H system was corroborated elsewhere.³⁵ In a very recent model, Robertson³³ has linked the H elimination reaction (in the H rich growth zone) to the strained (weak) bond distribution (overall network disorder), and suggested that plasma conditions (i.e., ion bombardment) can also affect the value of E_0 . We prefer to stick to the MGP model, but with an additional refinement. In the MGP model, certainly radicals with higher sticking coefficients (along with energetic particle bombardment) induce growth in a “noncrystalline morphology”—that is, growth exhibiting more film disorder.²⁵ And certainly growth by such radicals can, as suggested above, contribute not only to enhanced surface roughness but also to microvoid formation. In previous publications E_0 , obtained by photothermal deflection spectroscopy (PDS), was plotted for a variety of amorphous systems (a -Si:H, a -SiC:H, a -SiGe:H) versus not only the infrared microstructure fraction parameter R^* , but also the density deficiency (from flotation density measurements) as well as the SAXS microvoid volume fraction V_f .^{35–38} It is noted that these investigations covered a range of V_f 's (and E_0 's) much larger than that for the present films. Although the methodology used in those publications to obtain the E_0 values has since been greatly improved (i.e., the CPM technique yields significantly narrower E_0 's when both CPM and PDS measurements are made on the same device quality a -Si:H films),³⁹ the trends were nevertheless clear in that both plots yielded an increase in E_0 for all samples with an increase in microstructure measured either by infrared (IR), flotation, or SAXS. In the present case, since R^* is ~0 for all samples (Fig. 1), we now refer back to Fig. 6, where the CPM E_0 is plotted versus film R_d . While we caution that it is difficult to make an exact correlation between E_0 and the SAXS Q_N because of the directionality of the microvoids previously mentioned, the trends are clear here as well. That is, from a comparison of the data in Figs. 5 and 6, it is seen that both E_0 and the SAXS V_f increase rapidly at low R_d 's (~up to 40 Å/s), and are roughly constant with further increases in R_d . Based upon these correlations, we suggest that the large majority of these strained (weak) bonds (which

contribute directly to the higher E_0 values) lie on or near these microvoid surfaces.

While noting the precedence for this suggestion in the literature^{40,41} as well as the zero value of R^* for the present films,⁴² we comment that relating the presence of these strained (weak) bonds to microvoid surfaces also enables us to explain why the Urbach edge reflects an increased disorder with increasing microvoid V_f while the structural measurements do not. Phrased another way, why isn't the existence of such a large V_f (where at least some Si–Si bonds on the inner surfaces of the microvoids are weaker, and thus exhibit more disorder) reflected in more overall film disorder as measured by Raman and XRD? To answer this question, we consider the present high R_d a -Si:H material to be a void–substance composite⁴³ consisting of bulk regions with optimum order, and microvoid regions exhibiting more disorder on their surfaces; that is, excess disorder higher than that exhibited for the optimum compact, low deposition rate films (with $E_0 \sim 42$ mV).²¹ We further assume that if the number of weak (disordered) bonds on these microvoid surfaces is more than 10% of the total number of bonds, then Raman or XRD should detect a more disordered matrix. Following the argument advanced earlier for the a -SiC:H alloy,³⁵ it is easily seen, for elliptically shaped microvoids exhibiting (averaged) major and minor axis dimensions of 200 and 40 Å, respectively [see Fig. 5(b)], and comprising $\sim 2\%$ of the total sample volume, that the number of weak bonds (assumed to be within 1 monolayer on these microvoid surfaces) is much too small to be detected by either Raman or XRD, both of which sample all bonds. Only if we allow the weak bonds associated with these microvoids to extend well below the microvoid surfaces (some 10's of Å into the film bulk) would we expect to observe some effect on (broadening of) the Raman and XRD measurements.

In an argument similar to that used above, we suggest that it is also possible that the increase in the as-grown defect density (N_A) with film R_d (or the excess in N_A over its "minimal defect density" value of $2-3 \times 10^{15} \text{ cm}^{-3}$)²¹ is also due directly to the increase in SAXS V_f , and that these "excess" dangling bonds must also lie on or near the microvoid surfaces. From the equilibrium arguments presented by a variety of growth models, N_A must track E_0 ; therefore, if the increase in E_0 is caused by the increased microvoid volume fraction, then the increase in N_A also must be caused by the same mechanism. This argument is consistent with the CPM data seen in Fig. 6(a). In particular, the absorption α at 1.2 eV increases systematically with R_d , ranging from $\sim 0.1 \text{ cm}^{-1}$ at 5 Å/s,⁴⁴ to $0.3-0.6 \text{ cm}^{-1}$ for films deposited from 17 to 40 Å/s, and then finally to $1-2 \text{ cm}^{-1}$ for all films deposited at higher rates. Since the bulk ordering in the films, as probed by Raman and XRD, is invariant with increasing R_d , there is no reason *a priori* why the bulk regions of the films should suddenly contain more strained bonds as well as more defects. However, from the estimates of the microvoid surface bonds presented above it is clear, following this argument, that only a small fraction of the microvoid surfaces have incomplete reconstruction or unpassivated bonds, resulting in excess surface DB's.

Furthermore, it is interesting to note that the stabilized defect densities (N_B), measured by capacitance techniques on rudimentary devices deposited using identical deposition conditions, do not depend on the SAXS V_f . In a previous publication⁷ we showed that the N_B 's, measured using drive level capacitance profiling after either a 1000 h light soak under AM1 or under accelerated light soaking conditions, were invariant with respect to film R_d . That is, for films deposited in a wide range of R_d 's, from 5 to >130 Å/s, the N_B values ranged between 1.5 and $4 \times 10^{16} \text{ cm}^{-3}$ while, from Fig. 5, the SAXS V_f increased by more than a factor of 100.

A sizeable literature exists relating the SWE to the presence of microvoids. Carlson first presented a model involving the motion of H on the internal surfaces of microvoid surfaces,^{40,41} based on the assumption that holes can be trapped on weak Si–Si bonds existing near these surfaces. Osawa *et al.*⁴⁵ provided experimental evidence for this model by correlating an increased light-induced electron spin resonance spin density with the fractional H content evolved at low anneal temperatures; this evolving H was suggested to be clustered H bonded in some fashion (mono-, dihydride) on (interconnected) microvoid surfaces. Bhattacharya and Mahan²³ then showed, using R^* , that samples with more microstructure showed an increased light induced effect. No specific information about the exact nature of these microvoids was claimed in either publication. Other, more recent works continue to correlate the SWE with either SiH_2 or $(\text{SiH}_2)_n$ bonding.⁴⁶ In several recent reviews, film microstructure continues to play a key role in attempts to explain material stability.^{47,48}

The same arguments initially carried over to device degradation. Guha *et al.* deposited both devices and companion SAXS films at R_d 's ranging from 1.4 to 14 Å/s, and noted a correlation between an increased SAXS signal and a deterioration in device performance.⁴⁹ In particular, when the higher R_d films, containing larger microvoid V_f , were incorporated into device structures, these solar cells showed an increased degradation upon light exposure. The increasingly inferior behavior of the devices in their initial state with increasing SAXS V_f was also noted. It may be important to note that the size of the microvoids in these films were quite small (~ 9 Å in diameter). Yang *et al.*⁵⁰ reached a similar conclusion in a subsequent study in which the films (for SAXS measurements) and devices were deposited using different substrate temperatures (175 and 300 °C) and varying H_2 dilutions (low, high).

However, exceptions to these trends have since been noted. Williamson⁸ found that a -SiGe:H devices, deposited using high H_2 dilution and exhibiting an improved device stability, exhibited a strong SAXS signal. This was due to highly elongated and oriented features which were quite large. It was suggested that the highly oriented nature of the defects parallel to the charge transport direction in cells may not have a significant effect on cell performance. On the other hand, Yang *et al.*, while noting the deterioration in device performance with increased SAXS scattering (see above),⁵⁰ also measured the defect densities on companion films by CPM, and found that all i layers saturated at about

the same value ($\sim 3 \times 10^{16} \text{ cm}^{-3}$). No explanation was given for this behavior.

The present results would seem to corroborate the CPM results of Yang *et al.*,⁵⁰ but in a different system (that is, variations in film R_d 's and not H dilution). While not directly disputing the results of many articles linking the SWE with microvoids per se, two possibilities arise. First, as mentioned above, it is possible that the SWE may be more intimately linked with smaller microvoids (i.e., multivacancies)⁵¹ as opposed to larger microvoids, and the SAXS technique may not have the sensitivity to detect these very small microvoids in sufficient quantities if the larger microvoids are also present in the films.⁵² In particular, evidence for very small microvoids (i.e., multivacancies) in *a*-Si:H does exist in the literature,^{53,54} and several SAXS studies yield microvoid dimensions (diameters) ranging from extremely small and spherical ($\sim 10 \text{ \AA}$)⁴⁹ to quite large and elongated ($\sim 70 \text{ \AA} \times 1700 \text{ \AA}$).⁸ Thus, it may be possible that these large microvoids may be involved to a lesser extent in the SWE than the smaller, multivacancy-type ($\sim 10 \text{ \AA}$) microvoids.

Second, the nature of the microvoids themselves needs to be carefully examined. Normally, the presence of a sizeable SAXS V_f is accompanied by not only a low temperature H evolution peak (having a peak position at about $400 \text{ }^\circ\text{C}$ which is invariant with film thickness) but also a "sizeable" value for R^* (that is, significant dihydride and/or polyhydride bonding).^{35,36,55} However, the present films exhibit neither (Figs. 1 and 4). The lack of a "standard" (i.e., at $400 \text{ }^\circ\text{C}$) low temperature evolution peak is all the more surprising in view of the fact that the microvoids are elongated along the film growth direction. The lack of such a low temperature evolution peak may indicate, similar to the *a*-SiGe:H case discussed above, that the microvoids are isolated (not interconnected), and thus do not serve as fast transport paths for H_2 to get to the film surface. The other feature of interest concerns the value of R^* , which is definitely ~ 0 . This is the highest SAXS V_f observed to date for an *a*-Si:H film where no (minimal) SiH_2 and/or $(\text{SiH}_2)_n$ bonding is observed (see Fig. 1). This may suggest, while the weak bonds that contribute to the increase in E_0 and the as-grown defect densities N_A can still lie on the microvoid surfaces, that minimal bonded H may reside on these surfaces. In one respect, this minimal bonded H on these internal surfaces may not be surprising in view of the fact that film deposition has occurred at T_s 's near, or even above, that where surface desorption of hydrogen from (internal) surfaces takes place; that is, the H which would normally decorate these microvoid surfaces has already evolved during film deposition. However, this observation may be significant, because the lack of bonded H on these surfaces could explain not only the lack of a standard low temperature H evolution peak, but could also be an additional reason (aside from the microvoid size) for the "lack of participation" of these microvoids in the SWE.

We do acknowledge, however, that another interpretation may exist for the integrated SAXS intensity; that is, that the objects detected by SAXS are not microvoids per se, but are H-rich regions of nonzero electron density.⁸ Some support for this interpretation does exist in the literature.^{11,56,57} In

particular, for the present low R_d HWCVD films containing $\sim 2 \text{ at. } \%$ H, NMR results have shown that a large fraction of the film volume ($\sim 80\%$) contains minimal H, and that the H that is contained in the film is confined only to a small fraction (20%) of the total volume. Should such a film inhomogeneity not only exist in the present high R_d films but also contribute significantly to the SAXS intensity, then the SAXS V_f would be much larger than previously quoted [see Fig. 5(a)]. In addition, such an interpretation might also resolve the "peculiar" nature of the microvoids mentioned above; that is, questions relating to the lack of a low temperature H evolution peak and the zero value of R^* for a film with such a large SAXS V_f . However, we end this discussion with the following comment. That is, if the inhomogeneity were to be of similar proportions (80% of the film volume containing minimal H) for the present high R_d films, which typically contain more bonded H (6–8 at. %) than those mentioned above ($\sim 2 \text{ at. } \%$), then this would mean that the remaining 20% of the sample volume would contain $>25 \text{ at. } \%$ H. Were this to be true, then we would expect that a considerable $(\text{SiH}_2)_n$ bonding component would be observed in the IR,⁵⁸ and this we do not observe. Certainly this is an interesting area for future research.

CONCLUSIONS

The structure of HWCVD *a*-Si:H, deposited at rates in excess of 100 \AA/s , has been examined by a variety of techniques, including XRD, Raman spectroscopy, H evolution, and SAXS. As R_d is increased from 5 to $>140 \text{ \AA/s}$, we find that the SRO (from Raman), the MRO (from XRD), and the peak position of the H evolution peak are invariant with respect to R_d , and exhibit structure consistent with a state-of-the-art, compact *a*-Si:H material deposited at low R_d ($<10 \text{ \AA/s}$). The only exception to this behavior is the SAXS signal, which increases by a factor of ~ 100 over that for our best, low C_H films deposited at $\sim 5 \text{ \AA/s}$. We propose that the invariance of the short and medium range order can be explained by the MGP growth model, in which film growth is dominated by the highly mobile SiH_3 radical specie. At the same time, however, the present high R_d HWCVD growth takes place at high SiH_4 depletion. This in turn suggests that not all the Si that is evaporated from the filament (resulting from the SiH_4 decomposition) is "reacted away" in the gas phase, and that some small fraction of this highly reactive specie reaches the growing film surface. We suggest that it is this "minority component" of film growth that contributes to the large SAXS intensity that is observed at high R_d . While this increasing SAXS intensity is not reflected in measurements of the overall structural order, it does influence the film electronic structure (E_0, N_A). In particular, we argue that, since the overall structural order is invariant with film R_d , there is no reason *a priori* why the bulk regions of the films should suddenly contain more strained bonds as well as more defects. However, if these strained bonds and defects can be associated with (lie on or near) the microvoid surfaces, then we have a plausible reason for the increase in both E_0 and N_A with increasing microvoid density. Finally, we note the invariance of the saturated defect density versus R_d , and

discuss possible reasons why the increase in the microvoid density apparently does not play a role in the Staebler–Wronski effect for this type of material.

ACKNOWLEDGMENTS

The authors gratefully acknowledge the support of Q. Wang, E. Iwaniczko, R. S. Crandall, and H. Branz of the NREL *a*-Si:H group. The NREL work is supported by the U.S. Department of Energy under Contract No. DE-AC36-99GO10337.

- ¹ See, i.e., Mater. Res. Soc. Symp. Proc. **557**, 105 (1999); and papers within the “high deposition rate” section.
- ² S. Guha, NREL/SR-520-24723, 15 (1998).
- ³ S. J. Jones, X. Deng, T. Liu, and M. Izu, Mater. Res. Soc. Symp. Proc. **507**, 113 (1998).
- ⁴ A. H. Mahan *et al.*, Mater. Res. Soc. Symp. Proc. **507**, 119 (1998).
- ⁵ B. P. Nelson, R. S. Crandall, E. Iwaniczko, A. H. Mahan, Q. Wang, Y. Xu, and W. Gao, Mater. Res. Soc. Symp. Proc. **557**, 97 (1999).
- ⁶ B. P. Nelson, Y. Xu, A. H. Mahan, D. L. Williamson, and R. S. Crandall, Mater. Res. Soc. Symp. Proc. **609**, A22.8 (2000).
- ⁷ A. H. Mahan, Y. Xu, B. P. Nelson, J. D. Cohen, K. C. Palinginis, R. S. Crandall, and A. C. Gallagher, Appl. Phys. Lett. **78**, 3788 (2001).
- ⁸ D. L. Williamson, Mater. Res. Soc. Symp. Proc. **377**, 251 (1995).
- ⁹ A. H. Mahan, E. Iwaniczko, B. P. Nelson, R. C. Reedy, Jr., T. Unold, R. S. Crandall, S. Guha, and J. Yang, AIP Conf. Proc. **394**, 27 (1996).
- ¹⁰ A. Poruba, A. Fejfar, Z. Remes, J. Springer, M. Vanecek, J. Kocka, J. Meier, P. Torres, and A. Shah, J. Appl. Phys. **88**, 148 (2000).
- ¹¹ A. H. Mahan, D. L. Williamson, and T. E. Furtak, Mater. Res. Soc. Symp. Proc. **467**, 657 (1997).
- ¹² S. Guha, J. Yang, D. L. Williamson, Y. Lubianiker, J. D. Cohen, and A. H. Mahan, Appl. Phys. Lett. **74**, 1860 (1999).
- ¹³ D. L. Williamson, Mater. Res. Soc. Symp. Proc. **557**, 251 (1999).
- ¹⁴ D. Beeman, R. Tsu, and M. F. Thorpe, Phys. Rev. B **32**, 874 (1985).
- ¹⁵ A. J. M. Bernitsen, Ph.D. thesis, Utrecht University, 1993, p. 32.
- ¹⁶ W. Beyer and H. Wagner, J. Appl. Phys. **53**, 8745 (1982).
- ¹⁷ M. B. Schubert, H.-D. Mohring, E. Lotter, and G. H. Bauer, IEEE Trans. Electron Devices **36**, 2863 (1989).
- ¹⁸ Q. Wang, E. Iwaniczko, Y. Xu, B. P. Nelson, and A. H. Mahan, Mater. Res. Soc. Symp. Proc. **557**, 163 (1999).
- ¹⁹ W. Beyer (private communication).
- ²⁰ X. Liu, R. O. Pohl, and R. S. Crandall, Mater. Res. Soc. Symp. Proc. **557**, 323 (1999).
- ²¹ A. H. Mahan and M. Vanecek, AIP Conf. Proc. **234**, 195 (1991).
- ²² W. M. M. Kessels, Ph.D. thesis, Technical University of Eindhoven, 2000, p. 83.
- ²³ E. Bhattacharya and A. H. Mahan, Appl. Phys. Lett. **52**, 1587 (1988).
- ²⁴ R. A. Street, J. Kakalios, and T. M. Hayes, Phys. Rev. B **34**, 3030 (1986).
- ²⁵ A. C. Gallagher, Mater. Res. Soc. Symp. Proc. **70**, 3 (1986).
- ²⁶ A. Matsuda and K. Tanaka, J. Appl. Phys. **60**, 2351 (1986).
- ²⁷ J. Perrin, Y. Takeda, N. Hirano, Y. Takeuchi, and A. Matsuda, Surf. Sci. **210**, 114 (1989).
- ²⁸ E. C. Molenbroek, Ph.D. thesis, University of Colorado, Boulder, CO, 1995.
- ²⁹ E. C. Molenbroek, A. H. Mahan, and A. C. Gallagher, J. Appl. Phys. **82**, 1909 (1997).
- ³⁰ W. M. M. Kessels, A. H. M. Smets, D. C. Marra, E. S. Aydil, D. C. Schramm, and M. C. M. van de Sanden, Thin Solid Films **383**, 154 (2001).
- ³¹ A. C. Gallagher, Thin Solid Films (in press).
- ³² C. C. Tsai, J. G. Shaw, B. Wacker, and J. C. Knights, Mater. Res. Soc. Symp. Proc. **95**, 219 (1987).
- ³³ J. Robertson, J. Appl. Phys. **87**, 2608 (2000).
- ³⁴ M. Stutzmann, Philos. Mag. B **60**, 531 (1989).
- ³⁵ A. H. Mahan, A. Mascarenas, D. L. Williamson, and R. S. Crandall, Mater. Res. Soc. Symp. Proc. **118**, 641 (1988).
- ³⁶ A. H. Mahan, P. Menna, and R. Tsu, Appl. Phys. Lett. **51**, 1167 (1987).
- ³⁷ A. H. Mahan, D. L. Williamson, B. P. Nelson, and R. S. Crandall, Sol. Cells **24**, 465 (1989).
- ³⁸ A. H. Mahan, B. P. Nelson, R. S. Crandall, and D. L. Williamson, IEEE Trans. Electron Devices **36**, 2859 (1989).
- ³⁹ Compare, versus film H content, the CPM E_0 's in Ref. 21 with those obtained by PDS on identically prepared films, as quoted in A. H. Mahan, J. Carapella, B. P. Nelson, R. S. Crandall, and I. Balberg, J. Appl. Phys. **69**, 6728 (1991).
- ⁴⁰ D. E. Carlson, Appl. Phys. A: Solids Surf. **41**, 305 (1986).
- ⁴¹ See D. E. Carlson, in *Disordered Semiconductors*, edited by M. A. Kastner, M. J. K. Thomas, and S. R. Ovshinsky (Plenum, New York, 1987), p. 613.
- ⁴² From Ref. 40, the number of strained bonds on the microvoid surfaces is suggested to increase considerably if the microvoids are NOT hydrogenated.
- ⁴³ D. E. Aspnes, Proc. SPIE **276**, 188 (1981).
- ⁴⁴ The CPM curve for this film is not shown, but the absorption at 1.2 eV can be inferred from the value of N_A given in Ref. 21.
- ⁴⁵ M. Ohsawa, T. Hama, T. Akasaka, T. Ichimura, H. Sakai, S. Ishida, and Y. Uchida, Jpn. J. Appl. Phys., Part 2 **24**, L838 (1985).
- ⁴⁶ C. Manfredotti, F. Fizzotti, M. Boero, P. Pastorino, P. Polesello, and E. Vittone, Phys. Rev. B **50**, 18046 (1994).
- ⁴⁷ C. R. Wronski, Mater. Res. Soc. Symp. Proc. **467**, 7 (1997).
- ⁴⁸ H. Fritzsche, Mater. Res. Soc. Symp. Proc. **467**, 19 (1997).
- ⁴⁹ S. Guha, J. Yang, S. J. Jones, Y. Chen, and D. L. Williamson, Appl. Phys. Lett. **61**, 1444 (1992).
- ⁵⁰ J. Yang, X. Xu, and S. Guha, Mater. Res. Soc. Symp. Proc. **336**, 687 (1994); This article discusses mainly device degradation versus *i* layer film deposition conditions. The SAXS results for these *i* layers are given in Ref. 8.
- ⁵¹ M. Vanecek, Z. Remes, J. Fric, R. S. Crandall, and A. H. Mahan, Proceedings of the 12th European PV Solar Energy Conference, 1994, p. 354.
- ⁵² D. L. Williamson (private communication); it is well known that larger scattering features are weighted more heavily in SAXS intensity measurements.
- ⁵³ Z. Remes, M. Vanecek, A. H. Mahan, and R. S. Crandall, Phys. Rev. B **56**, R12710 (1997).
- ⁵⁴ See X. Zou, Y. C. Chan, D. P. Webb, Y. W. Lam, Y. F. Hu, C. D. Beling, S. Fung, and H. M. Weng, Phys. Rev. Lett. **84**, 769 (2000) and references therein.
- ⁵⁵ W. Beyer, Semicond. Semimet. **61**, 165 (1999).
- ⁵⁶ Y. Wu, J. T. Stephen, D. X. Han, J. M. Rutland, R. S. Crandall, and A. H. Mahan, Phys. Rev. Lett. **77**, 2049 (1996).
- ⁵⁷ D. Han, NREL Subcontract No. XAK-8-17619-11, Quarterly Report 8/15/00 (unpublished).
- ⁵⁸ A. H. Mahan (private communication); for the low R_d HWCVD films, any films containing typically >10 at. % total H, as measured by IR, exhibited a shifted stretch mode at 2090 cm^{-1} consistent with SiH_2 and/or $(\text{SiH}_2)_n$ bonding.